

LETTER TO THE EDITOR

On the Formation of Runaway Stars BN and x in the Orion Nebula Cluster

Juan P. Farias¹ and Jonathan C. Tan^{1,2}

¹ Dept. of Space, Earth & Environment, Chalmers University of Technology, Gothenburg, Sweden

² Dept. of Astronomy, University of Virginia, Charlottesville, VA 22904, USA

April 7, 2021

ABSTRACT

We explore scenarios for the dynamical ejection of stars BN and x from source I in the Kleinmann-Low nebula of the Orion Nebula Cluster (ONC), which is important for being the closest region of massive star formation. This ejection would cause source I to become a close binary or a merger product of two stars. We thus consider binary-binary encounters as the mechanism to produce this event. By running a large suite of N -body simulations, we find that it is nearly impossible to match the observations when using the commonly adopted masses for the participants, especially a source I mass of $7 M_{\odot}$. The only way to recreate the event is if source I is more massive, i.e., $\sim 20 M_{\odot}$. However, even in this case, the likelihood of reproducing the observed system is low. We discuss the implications of these results for understanding this important star-forming region.

Key words. methods: numerical — stars: formation — stars: kinematics and dynamics

1. Introduction

The Kleinmann-Low (KL) Nebula is a well-studied region in the Orion Nebula Cluster (ONC), being the closest, ≈ 400 pc (Menten et al. 2007; Kounkel et al. 2017) location where massive stars are forming. In particular, radio source I is likely to be a massive protostar (Churchwell et al. 1987; Garay et al. 1987). Close to the KL Nebula is the Becklin-Neugebauer (BN) object (Becklin & Neugebauer 1967). BN is a young, massive (8.0 – $12.6 M_{\odot}$, Scoville et al. 1983; Rodríguez et al. 2005) star, with fast 3D motion through the ONC of about 30 km s^{-1} , i.e., it is a “runaway” star. The origin of this motion has been a matter of debate. One scenario is that BN was dynamically ejected from the θ^1 Ori C system (now a binary) in the Trapezium grouping near the center of the ONC about 4,000 years ago (Tan 2004). This hypothesis has been supported with N -body simulations (Chatterjee & Tan 2012), which show several current properties of θ^1 Ori C, including orbital binding energy and recoil proper motion, can be understood to result from the ejection of BN.

An alternative scenario has been proposed by Bally & Zinnecker (2005) and Rodríguez et al. (2005) who suggested that dynamical interaction of BN, source I and perhaps an additional member, originally proposed to be radio source n, could have resulted in the high proper motions of BN and radio source I that are approximately in opposite directions. Details of this third member are crucial for this scenario since momentum conservation using BN and source I alone results in a mass for source I of $\sim 20 M_{\odot}$ in contrast to the $7 M_{\odot}$ estimations from gas motions near the source (Matthews et al. 2010; Hirota et al. 2014; Plambeck & Wright 2016).

Recent observations using multi-epoch high resolution near-IR images from the *Hubble Space Telescope* (HST) (Luhman et al. 2017) have shown high proper motion of another star, source x, that strongly indicate that it was the third member of the multiple system (see Figure 1). Given source x’s mass

($\sim 3 M_{\odot}$) and proper motion, now the mass estimation for source I via momentum conservation and from circumstellar disk gas dynamics are in better agreement at $\sim 7 M_{\odot}$. It has been also argued that if source I was a loose binary that merged during the interaction, e.g., 6 and $1 M_{\odot}$ stars, the released potential energy would be more than enough to explain the kinetic energy of the system.

However, there are some aspects of this scenario that appear questionable. In particular, it involves the most massive star, BN, being ejected as a single star from a binary of two much lower mass stars, i.e., with total mass of $\sim 7 M_{\odot}$. Thus in this paper we carry out numerical experiments to explore this scenario. We focus on the case where a binary source I (with components I_1 and I_2) interacted with another binary composed of BN and source x in a bound system that resulted in the dynamical ejection of source x and BN.

We present a set of $\sim 10^7$ pure N -body scattering simulations focused on the possible binary-binary interaction event that formed the observed system. We first test the scenario presented by Luhman et al. (2017) and then modify some of the parameters, especially source I’s mass, to test the sensitivity of the results. We describe our methods and initial conditions in §2, present our results in comparison to the observed system in §3 and discuss our findings and draw conclusions in §4.

2. Methods

We explore the scenario in which the ejection of BN and source x was caused by a dynamical decay of a multiple system that included source I, which was two stars in the past that may have merged as a result of the dynamical interaction. Ignoring situations with pre-existing triples and higher-order multiples that require large numbers of parameters for their description, three possible cases can be considered as initial conditions for this event involving four members. Case 1: a binary-binary inter-

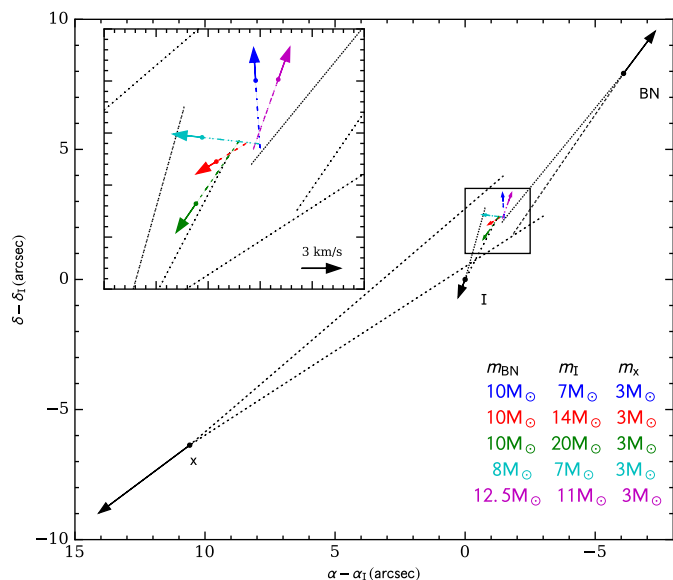


Fig. 1. Overview of the ejection scenario, also showing the center of mass motion given different combinations of masses explored in this work. Filled circles show actual positions of the stars and of the center of mass, dashed lines track the positions 540 years ago (1σ error cones shown for BN, I and x) and solid lines with arrows show 100 years into the future based on current proper motions in the rest frame of Orion (see Luhman et al. 2017). Different colors show various mass combinations of the stars that we have explored. Positions are relative to source I ($\alpha(J2000) = -05^{\text{h}}35^{\text{m}}14^{\text{s}}.516$ and $\delta(J2000) = -05^{\circ}22'30''.59$, Rodríguez et al. 2017).

action; Case 2: a binary system perturbed by two single stars; and Case 3: all stars were single stars. For simplicity we explore only the first case, which is arguably the most probable since it involves close interaction of only two initially independent systems. Cases 2 and 3 involve the coordinated close encounter of 3 and 4 systems, respectively, which makes them intrinsically less likely. Thus, we do not consider Cases 2 and 3 further in this letter.

Within Case 1 there are three possible initial combinations that we label as A: $[I_1 I_2][\text{BN } x]$; B: $[I_1 \text{BN }][I_2 x]$ and C: $[I_1 x][I_2 \text{BN}]$, where $[a b]$ indicates a binary pairing of stars a and b. We look for interactions that result in the outcome $[I_1 I_2]\text{BN } x$, i.e., with the ejection of BN and x leaving the binary $[I_1 I_2]$ with or without a merger, that we will refer to as BNx-ejection. From this subset of cases we identify those in which the velocities of the individual stars are within $2\text{-}\sigma$ of the observed values reported by Luhman et al. (2017) and Rodríguez et al. (2017) as BNx-velocity.

For our fiducial case, we adopt the same masses discussed by Luhman et al. (2017), i.e., $m_{\text{x}} = 3 M_{\odot}$, $m_{\text{BN}} = 10 M_{\odot}$ and $m_{\text{I}} = 7 M_{\odot}$ (Matthews et al. 2010; Hirota et al. 2014; Plambeck & Wright 2016). Assuming that source I was two stars, binary or not, we assume a mass ratio $q = 0.166$ for its members (i.e., $m_{\text{I}_1} = 6 M_{\odot}$ and $m_{\text{I}_2} = 1 M_{\odot}$), but we have also tested a range of other values finding no major change in the results due to this choice. The radius of the individual stars are taken from stellar models developed by Hurley et al. (2000). We assume I_1 and I_2 are protostars or pre-main-sequence stars and thus increase their radius by a factor $\eta \geq 1$ to account for the more extended radii that a protostar should have relative to a main sequence star of the same mass, adopting $\eta = 2$ as a simple, fiducial choice. We also test the sensitivity of our results to this factor finding no

major difference on the results except when this becomes ≥ 3 at which point the energy of ejections falls considerably.

Given the previous assumptions, there are then several combinations of parameters that set the initial conditions of each experiment. Our standard procedure is to choose them randomly from expected distributions, summarized as follows: (1) The semimajor axis a of each binary is taken from a uniform, random distribution in logarithmic space in the range $a = 0.1 - 6300$ AU. (2) The eccentricity of each binary is chosen using two extreme distributions: A) Using only circular orbits, i.e., $e_i = 0$, which might be expected if binaries formed via circumstellar disks; B) A thermal distribution (Heggie & Hut 2003), i.e., $dF_b/de = 2e$, which is the extreme scenario in which binary systems have had enough time to thermalize via stellar encounters. (3) The direction of the angular momentum vector of each binary is chosen randomly, as is (4) the initial orbital phase of the binaries. The above parameters define the internal properties of each binary.

Next come the parameters that define the interaction itself. We setup the experiments in order to only have initially bound systems, i.e., if both binaries were single stars they would remain bound after the interaction. Therefore, (5) the relative velocity at infinity v_i is drawn from a Maxwell-Boltzmann velocity distribution with $\sigma = 3 \text{ km s}^{-1}$ truncated at the critical velocity

$$v_c = \sqrt{\frac{G}{\mu} \left(\frac{m_{11}m_{12}}{a_1} + \frac{m_{21}m_{22}}{a_2} \right)}, \quad (1)$$

where G is the gravitational constant, $m_1 = m_{11} + m_{12}$ and $m_2 = m_{21} + m_{22}$ are the masses of each binary, summing their respective components, and $\mu = (m_1 + m_2)/(m_1 m_2)$ is the reduced mass of the system (see Gualandris et al. 2004). Thus v_c is the velocity below which the total energy of the system in the four body center of mass is negative, and therefore the ejected stars are the result of dynamical interaction and not of the initial conditions. Also, full ionization is not possible, i.e., there will be always a binary (or merged stars) left behind.

Next is: (6) the impact parameter, b , which is drawn randomly in discrete bins of radii $b_i = 2^{i/2} b_0$ following the method of McMillan & Hut (1996) to calculate cross sections of the relevant interactions. We choose $b_0 = 100$ AU and increase i until no relevant outcomes are encountered. Then, the contribution of the events in each bin i to the final cross section of this event Σ_X is $\pi(b_i^2 - b_{i-1}^2)N_{X,i}/N_i$ with $N_{X,i}$ and N_i being the number of events X and the number of trials respectively, both inside the i -th bin. The contribution of bin i to the squared uncertainty in the calculation, $(\delta\Sigma_X)^2$, is $[\pi(b_i^2 - b_{i-1}^2)/N_i]^2 N_{X,i}$ (McMillan & Hut 1996). For the first bin we have chosen $N_{i=1} = 500\,000$.

Simulations are performed using the Fewbody software (Fregeau et al. 2004), an accurate Runge-Kutta integrator which conserves energy and angular momentum to the order of 10^{-8} . It also uses the ‘‘sticky star’’ approximation for collisions with no mass loss and an expansion factor of the merger product of $f_{\text{exp}} = 2$.

The above method is repeated for different combinations of the member masses. All these combinations with their respective total momentum vectors are shown in Figure 1.

3. Results

Table 1 summarises the resulting interaction cross sections and branching ratios (BR), i.e. the number of cases over the total number of simulations for each configuration, for the

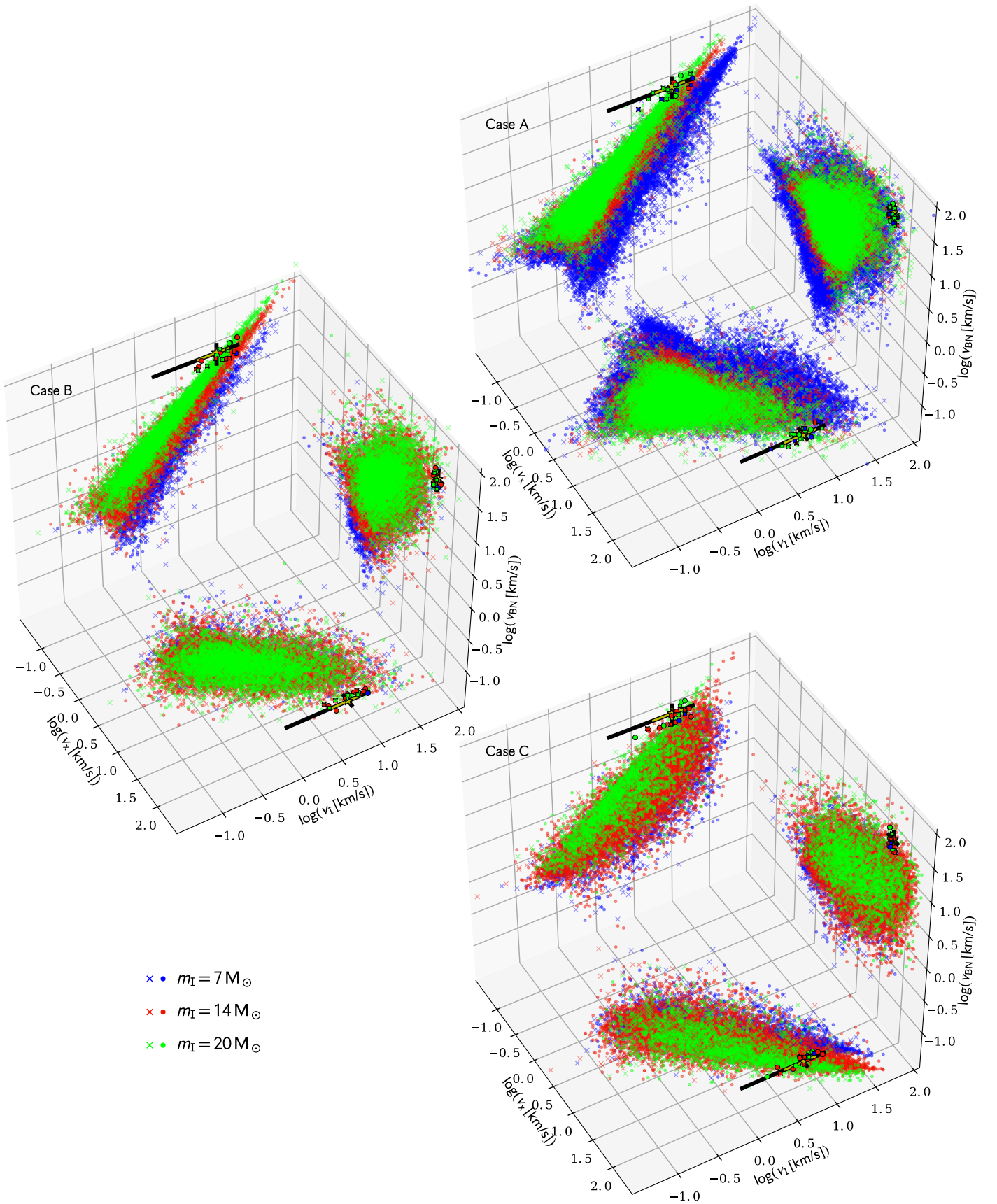


Fig. 2. Simulation results compared with observed velocities. Case A, Case B and Case C panels shows the resulting velocities that match the BNx-ejection event in the three velocity planes for sources I, x and BN for each respective initial combination varying only the mass of source I. Crosses and filled circles represent the adopted eccentricity distribution with thermal and circular eccentricities, respectively. Yellow star and errorbars shows the observed values with its standard error. Highlighted symbols represent BNx-velocity matches. Black errorbars shows the range on which BNx-velocity was searched, i.e., 2σ errors.

Table 1. Interaction cross sections for the different mass combinations

Case	Eccentricity	$m_1 [M_\odot]$	$m_{\text{BN}} [M_\odot]$	BNx-ejection		BNx-velocity		$N_{\text{sims}} [\times 10^6]$
				$\Sigma [\times 10^6 \text{AU}^2]$	BR $[\times 10^{-3}]$	$\Sigma [\text{AU}^2]$	BR $[\times 10^{-6}]$	
A	circular	7	10	2.82 ± 0.02	35.0	0.2 ± 0.2	0.392	5.10
A	thermal	7	10	1.84 ± 0.01	29.4	2 ± 2	1.17	5.11
A	circular	14	10	6.65 ± 0.04	39.4	16 ± 8	6.85	5.11
A	thermal	14	10	4.55 ± 0.03	32.9	11 ± 4	7.88	5.71
A	circular	20	10	9.95 ± 0.07	38.3	49 ± 9	31.8	6.09
A	thermal	20	10	6.72 ± 0.04	38.4	44 ± 10	25.1	5.71
A	circular	7	8	3.29 ± 0.02	37.5	0.5 ± 0.3	0.780	5.13
A	thermal	7	8	2.01 ± 0.02	35.2	1.0 ± 0.9	1.04	4.81
A	circular	7	12.5	2.37 ± 0.02	28.1	< 0.06	< 0.12	8.50
A	thermal	11	12.5	1.50 ± 0.01	25.5	0.8 ± 0.8	0.195	5.12
<hr/>								
B	circular	7	10	0.018 ± 0.002	0.240	0.06 ± 0.06	0.125	8.0
B	thermal	7	10	0.008 ± 0.001	0.208	< 0.06	< 0.13	7.5
B	circular	14	10	0.21 ± 0.01	4.53	1.5 ± 0.4	2.58	5.4
B	thermal	14	10	0.101 ± 0.004	3.87	2.1 ± 0.6	3.12	4.81
B	circular	20	10	0.53 ± 0.01	12.7	25 ± 14	13.7	5.41
B	thermal	20	10	0.293 ± 0.008	10.4	15 ± 2	16.8	5.12
B	circular	7	8	0.023 ± 0.001	0.458	0.06 ± 0.06	0.133	7.51
B	thermal	7	8	0.011 ± 0.001	0.347	0.2 ± 0.2	0.444	4.5
B	circular	11	12.5	0.018 ± 0.003	0.124	< 0.06	< 0.20	5.12
B	thermal	11	12.5	0.0069 ± 0.0008	0.111	< 0.06	< 0.13	7.40
<hr/>								
C	circular	7	10	0.017 ± 0.001	0.490	0.1 ± 0.1	0.125	8.01
C	thermal	7	10	0.011 ± 0.001	0.273	0.06 ± 0.06	0.125	8.01
C	circular	14	10	0.045 ± 0.002	1.35	3 ± 2	0.823	8.51
C	thermal	14	10	0.043 ± 0.004	1.34	4 ± 1	3.13	5.12
C	circular	20	10	0.083 ± 0.004	2.15	51 ± 18	8.21	5.12
C	thermal	20	10	0.081 ± 0.005	2.66	36 ± 16	8.67	5.42
C	circular	7	8	0.020 ± 0.001	0.847	0.1 ± 0.1	0.133	7.51
C	thermal	7	8	0.012 ± 0.001	0.494	0.13 ± 0.09	0.266	7.51
C	circular	11	12.5	0.011 ± 0.001	0.281	0.1 ± 0.1	0.222	4.51
C	thermal	11	12.5	0.011 ± 0.002	0.141	< 0.06	< 0.20	5.11

BNx-ejection and BNx-velocity cases. The interaction cross sections of the BNx-ejection case are considerably larger for Case A, with $\Sigma_{\text{BNx-ejection}} = (2.8 \text{ and } 1.8) \times 10^6 \text{AU}^2$ for the fiducial (i.e., $m_{\text{BN}} = 10 M_\odot, m_1 = 7 M_\odot, m_x = 3 M_\odot$) circular and thermal cases, respectively. Such large cross sections, together with branching ratios of several percent of the BNx-ejection event in the fiducial case that we show in Figure A.1 and discuss further in Appendix A, implies that the ejection of the massive BN object and source x from the system is quite possible.

However, when considering the velocities of the ejected stars in the BNx-velocity case, the cross sections drop to $\sim 1 \text{AU}^2$ in all fiducial cases. We have checked that this result is independent of the assumed mass ratio of the source I components. Also, if η is greater, then the chance of obtaining the observed velocities becomes even smaller, due to the energy constraints that the radii of the stars imply. We have found that to match the observed velocities the parameter η must be no larger than 3, i.e., for a given mass, the protostars should not have radii larger than 3 times the radii of a main sequence star of the same mass.

The situation becomes more favorable only if the mass of source I is $> 7M_\odot$. In the best case we explored, with $m_1 = 20M_\odot$ cross sections increase by a factor between ~ 20 to 600 in the different initial configurations. However, the cross sectional areas are still small, ~ 10 to 50AU^2 , which means that these events are quite rare when compared to the whole ensemble of outcomes. In Appendix A we present and discuss the branching ratios of all

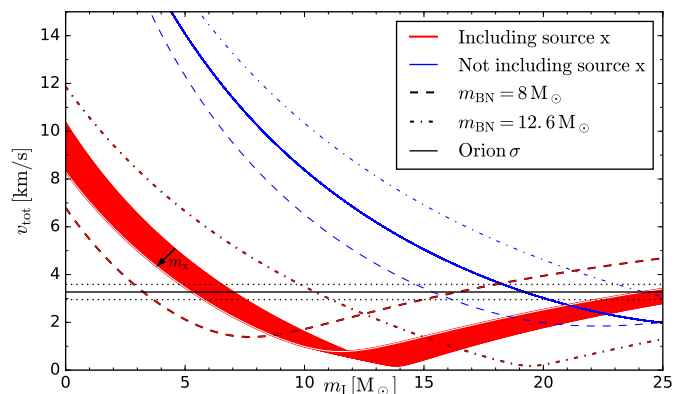


Fig. 3. The system (center of mass) velocity as a function of the mass of source I (see also Figure 1). Red lines show the scenario where source x is part of the ejection event as suggested by Luhman et al. (2017)¹. The red shaded area shows the result of varying the mass of source x between 2.5-3.0 M_\odot , with the black arrows showing the direction of the increment. Blue lines show the scenario if source x was not part of the event. In both red and blue cases, the dashed and dot-dashed lines show results of adopting the lower and upper limits of BN's mass, respectively (Rodríguez et al. 2005).

¹ Note that there is an error in the units for the velocity associated with the specific momentum that they mention: it should be 1.4mas yr^{-1} instead of km s^{-1} .

the possible outcomes of our experiments sorted from the most to least probable.

4. Discussion and Conclusions

Our simulations indicate that a more massive source I has a better chance to produce the observed system. Figure 2 shows a scatter plot of the velocities obtained in each setup when varying source I's mass. The yellow star and errorbars show the observed system. There is a very specific trend that appears in the $v_{\text{BN}} - v_{\text{I}}$ panels in Figure 2 showing that the observed system appears to be one order of magnitude above the trend for source I that has a mass of $7 M_{\odot}$. Increasing source I's mass naturally places simulations in agreement with observations. Even though we have shown this type of event is quite rare in terms of branching ratios with respect to all possible outcomes, if by chance it happens with the correct released energy, the observed velocities would be only achieved if the mass of source I is not so small. This is also supported by the other velocity panels in all the Cases A, B and C.

Some caveats associated with our analysis should be mentioned. For example, we have ignored the dynamical effects of gas expulsion. The modeling of Chernoff et al. (1982) implies about $4 M_{\odot}$ of gas has been ejected from the central region over a period of 1200 years requiring an energy of $\gtrsim 5 \times 10^{47}$ erg. If a large fraction of this gas was ejected impulsively at the time of dynamical interaction, then this could alter some of the specific results of our analysis: e.g., an even greater energy needs to be liberated in the dynamical interaction. However, we note that the gas has been ejected quasi-isotropically from BN-KL (see, e.g., Allen & Burton 1993; Bally et al. 2017), so that the effects on the plane-of-sky momentum analysis are not expected to be so large. Still, future modeling could allow for, e.g., a variable mass of stars during the interaction, i.e., sudden mass loss occurring as part of any merger event. Other caveats include that we have ignored the dynamical effects of any other masses, including other surrounding stars and gas components. Still, these are expected to be relatively minor since the velocities of the stars are relatively large compared to the velocity dispersion of the ambient material in the region.

The recent evidence that source x was involved in the ejection of the BN Object appeared to reconcile the incongruence between the mass of source I estimated by momentum analysis and estimations via rotation of its putative circumstellar disk. However, if we re-do momentum analysis with the new data we can see that source x's participation is not enough support for the low mass estimations of source I. Figure 3 shows the momentum analysis for the old and new scenarios as a function of source I mass. Blue lines shows the scenario where only source I and BN participated in the ejection with the upper and lower limits of BN's mass as dashed lines. The only way the system center of mass can be moving within the velocity dispersion of the ONC (black solid line) is if source I's mass is at least $20 M_{\odot}$. Now, it has been argued that the inclusion of source x would remove this constraint. The former is true as we can see in the red lines on Figure 3, however, for the system to be moving within the velocity dispersion of the ONC, source I's mass could actually be in a very wide range of masses, from 5 to $25 M_{\odot}$ with a minimum near $14 M_{\odot}$.

Figure 1 shows the present center of mass with different mass combinations used in this work. If the individual masses are those adopted by Luhman et al. (2017) (blue arrow) the system is moving mostly outwards, away from the center of the ONC. However, if source I is more massive (red and green arrows) the

system velocity points towards the center of the cluster, i.e., towards the Trapezium. We consider that a scenario involving infall of a dense molecular gas core from which the protostars are forming is more likely than one involving motion of the core out from the cluster center. For example, passage near the strong ionizing radiation from $\theta^1\text{C}$ is expected to have had potentially very disruptive effects on the core if it had previously been located near the Trapezium.

In conclusion, we have shown that the ejection of BN and x from source I (as a binary or merged binary) as presented by Luhman et al. (2017), i.e., with a relatively low mass for source I of $\sim 7 M_{\odot}$ that is less than BN's mass, is in general a very unlikely event. In particular, with the given masses and observed velocities it is nearly impossible to reproduce the observations with the binary-binary interactions we have considered. If the interaction occurred as we have explored, then it is more probable that source I is much more massive than the preferred value of $7 M_{\odot}$ presented by Luhman et al. (2017) and others. Thus future measurements of the mass of source I are needed to better constrain this proposed ejection scenario.

However, other possible initial combinations remain to be explored, e.g., a binary perturbed by two stars (i.e., effectively a 3-body initial interaction), or all initial single stars (i.e., a 4-body initial interaction), but these are expected to be inherently rarer and there is no reason to think these combinations could increase the chances significantly since the binary-binary interaction is the most likely to release the necessary energy to produce the ejection. A single star interacting with a pre-existing triple remains a possibility that needs to be considered, especially if the dynamical mass of source I does turn out to be at the low end of the range modeled, i.e., $\sim 7 M_{\odot}$. Such interactions could also include unbound fly-bys. This would be the only way to reconcile the scenario of BN's ejection from $\theta^1\text{C}$ (Tan 2004; Chatterjee & Tan 2012) with ejection of source x, although plane-of-sky momentum conservation would appear to place challenging constraints on such a model if BN suffered only minor accelerations and course deflections in such a fly-by.

References

- Allen, D. A. & Burton, M. G. 1993, *Nature*, 363, 54
 Bally, J., Ginsburg, A., Arce, H., et al. 2017, *ApJ*, 837, 60
 Bally, J. & Zinnecker, H. 2005, *AJ*, 129, 2281
 Becklin, E. E. & Neugebauer, G. 1967, *ApJ*, 147, 799
 Chatterjee, S. & Tan, J. C. 2012, *ApJ*, 754, 152
 Chernoff, D. F., McKee, C. F., & Hollenbach, D. J. 1982, *ApJ*, 259, L97
 Churchwell, E., Felli, M., Wood, D. O. S., & Massi, M. 1987, *ApJ*, 321, 516
 Fregeau, J. M., Cheung, P., Portegies Zwart, S. F., & Rasio, F. A. 2004, *MNRAS*, 352, 1
 Garay, G., Moran, J. M., & Reid, M. J. 1987, *ApJ*, 314, 535
 Gualandris, A., Portegies Zwart, S., & Eggleton, P. P. 2004, *MNRAS*, 350, 615
 Heggie, D. & Hut, P. 2003, *The Gravitational Million-Body Problem: A Multi-disciplinary Approach to Star Cluster Dynamics*
 Hirota, T., Kim, M. K., Kurono, Y., & Honma, M. 2014, *ApJ*, 782, L28
 Hurley, J. R., Pols, O. R., & Tout, C. A. 2000, *MNRAS*, 315, 543
 Kounkel, M., Hartmann, L., Loinard, L., et al. 2017, *ApJ*, 834, 142
 Luhman, K. L., Robberto, M., Tan, J. C., et al. 2017, *ApJ*, 838, L3
 Matthews, L. D., Greenhill, L. J., Goddi, C., et al. 2010, *ApJ*, 708, 80
 McMillan, S. L. W. & Hut, P. 1996, *ApJ*, 467, 348
 Menten, K. M., Reid, M. J., Forbrich, J., & Brunthaler, A. 2007, *A&A*, 474, 515
 Plambeck, R. L. & Wright, M. C. H. 2016, *ApJ*, 833, 219
 Rodríguez, L. F., Dzib, S. A., Loinard, L., et al. 2017, *ApJ*, 834, 140
 Rodríguez, L. F., Poveda, A., Lizano, S., & Allen, C. 2005, *ApJ*, 627, L65
 Scoville, N., Kleinmann, S. G., Hall, D. N. B., & Ridgway, S. T. 1983, *ApJ*, 275, 201
 Tan, J. C. 2004, *ApJ*, 607, L47

Appendix A: Branching ratios for all the possible outcomes

By calculating interaction cross sections for the BNx-ejection case we have obtained a large number of interactions on the order of a few millions per simulation set with impact parameters from near zero to as large thousands of AU, by which point no interesting interaction happens. With this large set of simulations we can calculate branching ratios of rare interactions down to $\sim 10^{-6}$. We have classified the outcomes of each experiment using a similar classification as Fregeau et al. (2004), however we distinguish the cases where there was an exchange of members or a capture of one of the members by one of the binary systems. Figure A.1 shows all the possible outcomes in this study sorted from the most to the least probable in our fiducial case with circular orbits. This trend is similar for the setups with thermal eccentricities. Figure A.1 shows that these models with thermal eccentricities have a greater chance to obtain a merger, but not in outcomes that could form the observed BN-x-I system.

In all setups, the most probable case is preservation i.e., the configuration of each setup does not change, happening $\sim 50\%$ of the time, followed by the “Triple+Single” case, i.e., the formation of a stable triple by capturing one member of the other binary ($\sim 20\%$). Our case of interest for Case A, i.e., “2 Singles+Binary”, comes in third place happening $\sim 10\%$ of the time. $[I_1 I_2]BN x$ is a subset of this case. The branching ratio of this specific subset is marked with the same symbol connected by a line to the parent set in Figure A.1. The end of the line shows the branching ratio of the subset that also match the observed velocities within 2σ . A left triangle marking the end of the line means that we did not find any velocity match for this case and the branching ratio is smaller than the position of the symbol. The branching ratio of $[I_1 I_2]BN x$ is quite high ($\sim 4.5\%$), this means that the case where the most massive star (BN) is ejected is not so rare. However, it is almost impossible to match the observed velocities in this particular case with the masses assumed by Luhman et al. (2017). Increasing the mass of source I considerably improves the chances to obtain the observed velocities, going from a branching ratio of $< 4 \times 10^{-7}$ i.e., not a single case with $m_1 = 7 M_\odot$ to a branching ratio of $\sim 2 \times 10^{-5}$ for $m_1 = 20 M_\odot$ (with $m_{I_1} = 17.14 M_\odot$ and $m_{I_2} = 2.86 M_\odot$).

The matching outcome for Cases B and C without a merger involves an exchange of members, which makes the outcome less frequent, but still comparable with the original case. The mass of source I also influences the branching ratios of the matching velocity outcomes, favoring the cases where source I is more massive.

This trend also remains the same when considering a merger between I_1 and I_2 , see the “3 Singles” case in Fig. A.1. Even though the branching ratios of these cases are smaller, the chances of obtaining the matching velocities are higher since it is the extreme case where most of the potential energy stored by the binary is released to the system members. How much energy is set by the semimajor axis and also individual radius of the source I original stars. For this situation, the radii of the protostars, parameterized by the factor η , is one of the largest unknowns in the system and one of the most important, since it sets the upper limit on the amount of energy the source I merger can provide.

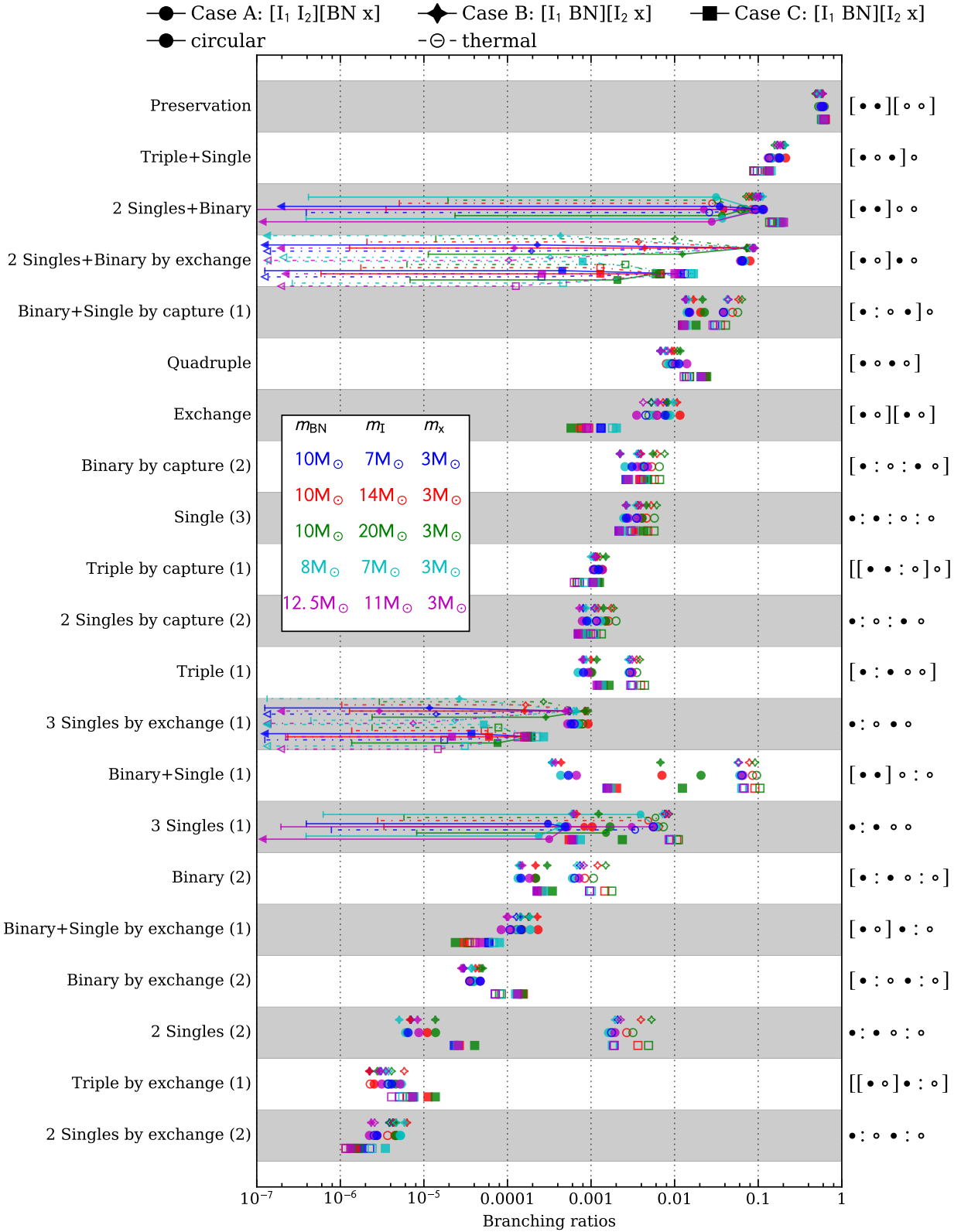


Fig. A.1. Branching ratios collected for all possible outcomes and experiments carried out in this work. Results are sorted from the most to the least probable in the fiducial case (blue filled circle). Different symbols represent the different initial configurations: Case A (circles); Case B (diamonds); and Case C (squares). Open symbols show cases with thermal distribution of eccentricities, while filled symbols show where all binaries have circular orbits initially. Colors show the different assumed masses (see legend). Left axis labels are the names used to refer to each outcome with the number of collisions needed for each outcome appearing in parentheses. Right labels show the schematic representation of each outcome, similar to Fregeau et al. (2004), but we distinguish between exchange of members or preservation of membership of the original binaries. Branching ratios of cases that match the BN-x-I observed configuration are a subset of some of the listed outcomes, these are connected to their parent outcome by a line (dashed for open symbols, solid for filled symbols). We mark outcomes where no matching velocity was found with a left triangle denoting the upper limit of their branching ratio. Thus only the outcomes that contain horizontal lines have some chance of producing the observed BN-x-I system, although typically we only have upper limits on the branching ratio that leads to the observed system.